



Quantifying erosion rates and stability of bottom sediments at mussel aquaculture sites in Prince Edward Island, Canada

Tony R. Walker^{a,b,*}, Jon Grant^a

^a Department of Oceanography, Dalhousie University, Halifax, Nova Scotia, Canada B3H 4J1

^b Dillon Consulting, 137 Chain Lake Drive, Halifax, Nova Scotia, Canada B3S 1B3

ARTICLE INFO

Article history:

Received 30 March 2008

Received in revised form 19 July 2008

Accepted 21 July 2008

Available online 26 July 2008

Keywords:

Microbial mats

Sediment stabilization

Sediment erosion rates

Resuspension

Mussel aquaculture

Tracadie Bay

ABSTRACT

Downward fluxes of organic biodeposits under suspended mussel culture cause benthic impacts such as microbial mat production. Quantifying sediment erosion in these coastal ecosystems is important for understanding how fluxes of organic matter and particulates contribute to benthic–pelagic coupling. Critical shear velocity (u^*), erosion rates and particle size distributions of resuspended sediment were measured at two sites; an impacted muddy site with extensive mussel culture (site 1), and a coarser sandier site with less mussel influence (site 2), using a new method for assessing sediment erosion at Tracadie Bay, Prince Edward Island in August 2003. Shear forces were generated by vertically oscillating a perforated disc at controlled frequencies. These forces correspond to shear velocity, using a re-designed and calibrated Particle Erosion Simulator. Undisturbed sediment cores obtained by divers and grab (sub-cored using a Plexiglas™ cores) were exposed to shear stress to compare differences between collection methods. Microbial mats were present at site 1 which initially biostabilized sediment against erosion due to ‘armor’ of the sediment, but onset of erosion was abrupt once these mats failed. Erosion sequences at site 2 (without mat cover) were smoother resulting in less material being eroded. Mean mass of material eroded was 47 and 23 g m^{−2} min^{−1} at sites 1 and 2 respectively. Mat area cover and shear velocity was strongly related. Critical shear velocities varied between 1.70 and 1.77 cm s^{−1}, with no obvious differences between location or collection method, so sediments from these two contrasting sites had identical mean critical shear velocities. Significant differences existed in the concentrations of chlorophyll *a*, colloidal and bulk carbohydrates, between mats and bare sediment from site 1. Particle sizes measured by videography of resuspended sediment at different shear velocities ranged from 100 μm (the minimum diameter capable of being detected by the system), to large mat fragments of 1700 μm for both sites. These results provide evidence of the relevance of using a portable erosion device to indicate how sediment erodability is affected by mussel–microbial relationships.

© 2008 Elsevier B.V. All rights reserved.

1. Introduction

Suspended mussel aquaculture produces high rates of biodeposition in coastal ecosystems because filter-feeding bivalves repackage fine suspended material into larger biodeposits (feces and pseudofeces) that are organically rich. These large deposits sink rapidly, increasing the flux of organic matter to the benthos (Chamberlain et al., 2001).

While the dynamics of mussel biodeposition (settling velocity, disaggregation rate and resuspension) are poorly quantified, enhanced sedimentation under mussel culture is well documented (e.g. Hatcher et al., 1994; Callier, et al., 2006). The downward flux and recycling of organic biodeposits under suspended mussel culture operations has been shown to have local benthic impacts which decreases biodiversity and increases anaerobic conditions and presence of microbial mats (Stenton-Dozey et al., 1999; Newell, 2004).

Increased sediment stability is often associated with microbial mats (Grant et al., 1986; Grant and Gust, 1987; Madsen et al., 1993); and is mainly a result of the excretion of

* Corresponding author. Dillon Consulting, 137 Chain Lake Drive, Halifax, Nova Scotia, Canada B3S 1B3. Tel.: +1 902 450 4000; fax: +1 902 450 2008.
E-mail address: tonyrobertwalker@gmail.com (T.R. Walker).

extracellular polymeric substances (EPS) by diatoms and/or bacteria, which physically bind cohesive and non-cohesive sediment particles (Paterson et al., 1990) and influences the exchange of particles between sediment and water column (Sutherland et al., 1998a,b). Microbial biomass (e.g. chlorophyll *a* pigment content) has been shown to correlate with sediment stability (Lelieveld et al., 2003; Lucas et al., 2003) and similar relationships have been established with colloidal carbohydrates (Dade et al., 1990).

Sediment erosion and stability is affected by many factors such as: biostabilization, porosity, organic content, grain size, and bioturbation (e.g. Paterson, 1989; Grant and Emerson, 1995; Lelieveld et al., 2004), therefore, quantifying sediment transport and erosion thresholds in coastal systems becomes an important predictive tool in order to understand fluxes of organic matter, particulates and associated contaminants (Watts et al., 2003). Calculating movement of marine sediments is only possible when the erosional response of the sediment to shear velocity is known, but is difficult because few calibrated data exists about entrainment rates of sediment especially those carpeted by microbial mats or those impacted by bivalve biodeposits (Sutherland et al., 1998b; Widdows et al., 1998; Tolhurst et al., 2000).

Measurements of critical shear stress and erosion rates of undisturbed cohesive sediments beneath suspension-feeding bivalves has rarely been investigated and is notoriously difficult to predict due to varying biotic and physical influences causing sediment to behave like a fabric rather than as discrete particles (Giles and Pilditch, 2004). Biodeposits interact with microbial mats to produce a bottomscape resulting from post-depositional processes, and resuspension of these particles will be affected by their source beds (microbial mats or bare sediment). There is a significant deficiency in predicting these benthic–pelagic exchanges at sites with extensive mussel culture.

To investigate the above we re-designed and calibrated a portable oscillating grid erosion device, Particle Erosion Simulator (PES) allowing quantification of erosion and resuspension parameters within natural sediment cores. The erosion device is also known as the Benthic Environmental Assessment Sediment Tool (BEAST) (see Walker et al., in press). In this paper results of these erosion studies are presented, including consideration of disturbance artifacts arising from core collection and handling. The following objectives were met at contrasting aquaculture sites within Tracadie Bay in Prince Edward Island (PEI), Canada: (a) quantify critical shear stress and erosion rate of bottom sediments; (b) determine particle size distribution of resuspended aggregates and their relationship to bottom shear; (c) determine effects of sediment quality (e.g. microbial mats) on erosion parameters; and (d) compare erosion features in cores collected by diver versus those collected by an Ekman grab.

2. Materials and methods

2.1. Sample collection

Tracadie Bay is a shallow bar-built estuary under intensive mussel culture (Meeuwig et al., 1998). Tidal currents pass through a narrow inlet, which exchanges the entire volume of the Bay every 4–10 days (Dowd, 2005). A deltaic sand body

with extensive *Zostera marina* (Eelgrass) beds bifurcate incoming channels within the inlet and Winter River enters the bay at its mid-point, providing is a limited source of freshwater. Various aspects of the benthic ecology of this Bay have previously been described by Shaw (1998). Two contrasting sampling sites were chosen in Tracadie Bay (Fig. 1). Site 1 located directly beneath mussel long lines was characterized by muddy sediments, patchy microbial mats of white sulfur bacteria and cyanobacteria and contained limited macro-fauna. Site 2 was characterized by sandier sediments, higher numbers of bioturbating macro-fauna, and no microbial mats.

At both sites sediment was collected using Plexiglas™ cores (40 cm long × 11 cm diameter, 98 cm² sediment surface) by SCUBA divers during August 2003. At site 1, additional cores were collected using an Ekman grab (Wildco®) with surface dimensions of 23 × 23 cm. Flaps on the grab at the top of the box closed as the core was pulled out of the sediment limiting the disturbance of the sediment bed. Surface seawater in the grab was allowed to drain away to minimize disturbance of the surface sediment before sub-coring. A Plexiglas™ core was taken for erosion experiments from each grab. Bottom caps with an o-ringed PVC plate were inserted beneath the new partially filled sediment-filled cores. On shore, cores were gently filled with approximately 2 L of ambient seawater. A floating plastic disc overlying the sediment surface eliminated disturbance of the bed. Each core was then stored in the dark in a water bath to equilibrate to *in situ* temperature before erosion experiments were performed. Triplicate mini-cores were collected over the 0–1 cm depth horizon with truncated 5 mL plastic syringes from separate diver cores for measurements of porosity, grain size, organic content, particulate nitrogen, total organic carbon (TOC), chlorophyll *a* and carbohydrates. Porosity samples were stored in pre-weighed plastic scintillation vials in a refrigerator until measurements were made as weight loss upon drying at 60 °C. Other samples were stored frozen at –20 °C until analysis.

Sediment grain size was analyzed using protocols according to Grant et al. (2002). For each site a thawed sample was gently shaken and wet sieved with tap water through a series of 63 to 2000 µm sieves, with a sub-sample of the <63 µm effluent collected and filtered. This gentle treatment preserves biogenic components. Surface samples (0–1 cm) of sediment organic content were oven dried at 60 °C and ashed in a furnace oven at 520 °C for 24 h before being re-weighed. Sediment for TOC and nitrogen analysis was measured in a CHN elemental analyzer (Perkin-Elmer 2400) with no pre-treatment (Walker, 2005).

2.2. Sedimentary carbohydrates and chlorophyll *a*

Sediment carbohydrate concentrations were determined by using a phenol–sulfuric acid method (see Grant et al., 1986). The extraction process was modified for analysis of carbohydrates in marine sediments by using a 30-ppt saline solution. After an extraction period of 1 h the sediment samples were centrifuged at 2000 rpm for 10 min to separate the sample into ‘colloidal’ and ‘bulk’ carbohydrate fractions. Colloidal carbohydrates are an index of EPS produced by diatoms. The sediment in the tube was also analyzed to calculate bulk carbohydrates. Calibrations were carried out

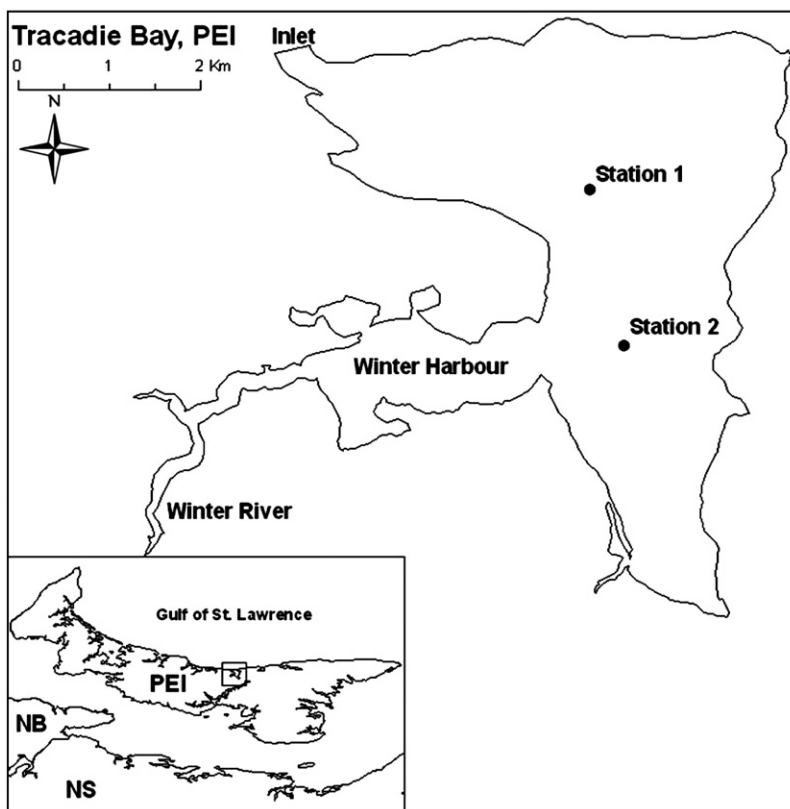


Fig. 1. Sampling sites in Tracadie Bay, Prince Edward Island, Canada.

with a range of glucose concentrations and carbohydrates expressed as glucose equivalents (Lucas et al., 1981). Frozen sediment samples for chlorophyll *a* analysis were thawed and extracted in 90% acetone then analyzed fluorometrically according to the procedure described by Lorenzen (1967). Two drops of 10% HCl were added to each sample and the fluorescence was converted to chlorophyll *a* following the method of Parsons et al. (1984).

2.3. Erosion experiments

The PES is a portable device originally devised by Tsai and Lick (1986) and used for testing undisturbed sediment cores. We have recently re-designed and calibrated this device for use as an inexpensive portable field instrument (see Walker et al., submitted for publication). An oscillating grid in the PES generates turbulence above the sediment which will exceed

Table 1

Summary of environmental data at sampling sites in Tracadie Bay, Prince Edward Island

Site	Co-ordinates	Depth (m)	Mean density (g mL ⁻¹)	Mean porosity (%)	Organic content (%)	TOC (%)	C/N ratio	Percentage grain size (μm)	Principle benthic characteristics	Mean critical shear velocity (cm s ⁻¹)
1	46° 23' 963 N 62° 59' 902 W	4.8	1.11 (0.06)	70 (0.08)	10.78 (0.01)	4.32 (0.18)	7.81 (0.09)	0.40 (2000) 0.71 (1000) 3.33 (500) 9.88 (250) 33.44 (125) 34.45 (63) 17.80 (<63)	Patchy microbial mats (e.g. <i>Beggiatoa</i>), limited macro-fauna, muddy sand (D_{50} = 120 μm)	1.74 (0.06) Diver and grab cores
2	46° 23' 193 N 62° 59' 555 W	4.1	1.52 (0.20)	77 (0.10)	3.42 (0.20)	1.19 (0.15)	7.32 (0.28)	19.45 (2000) 2.61 (1000) 1.86 (500) 39.38 (250) 25.75 (125) 1.03 (63) 9.93 (<63)	No microbial mats, more macro-fauna and bioturbation, mussel shell fragments, sand (D_{50} = 316 μm)	1.75 (0.07)

Values represent means (±SE, n = 3–12).

its critical threshold as oscillation frequency is increased. The mechanical aspects of the erosion device were slightly altered, but the dimensions of the erosion chamber and oscillating disc were true to the original. The oscillating disc is located at a minimum of 2–3 cm from the sediment bed and has an excursion of 2.54 cm. The flow characteristics of the PES have been quantified using a stress sensor, allowing expression of

grid oscillation in terms of shear velocity u^* (Walker et al., submitted for publication). Although we do not provide calibration data herein we have verified that motor speed and shear velocity have a linear relationship such that the erosion measurements reported below can be inter-compared regardless of PES calibration. The perforated plunger disc was inserted into the core, and oscillation imposed for 2 min erosion

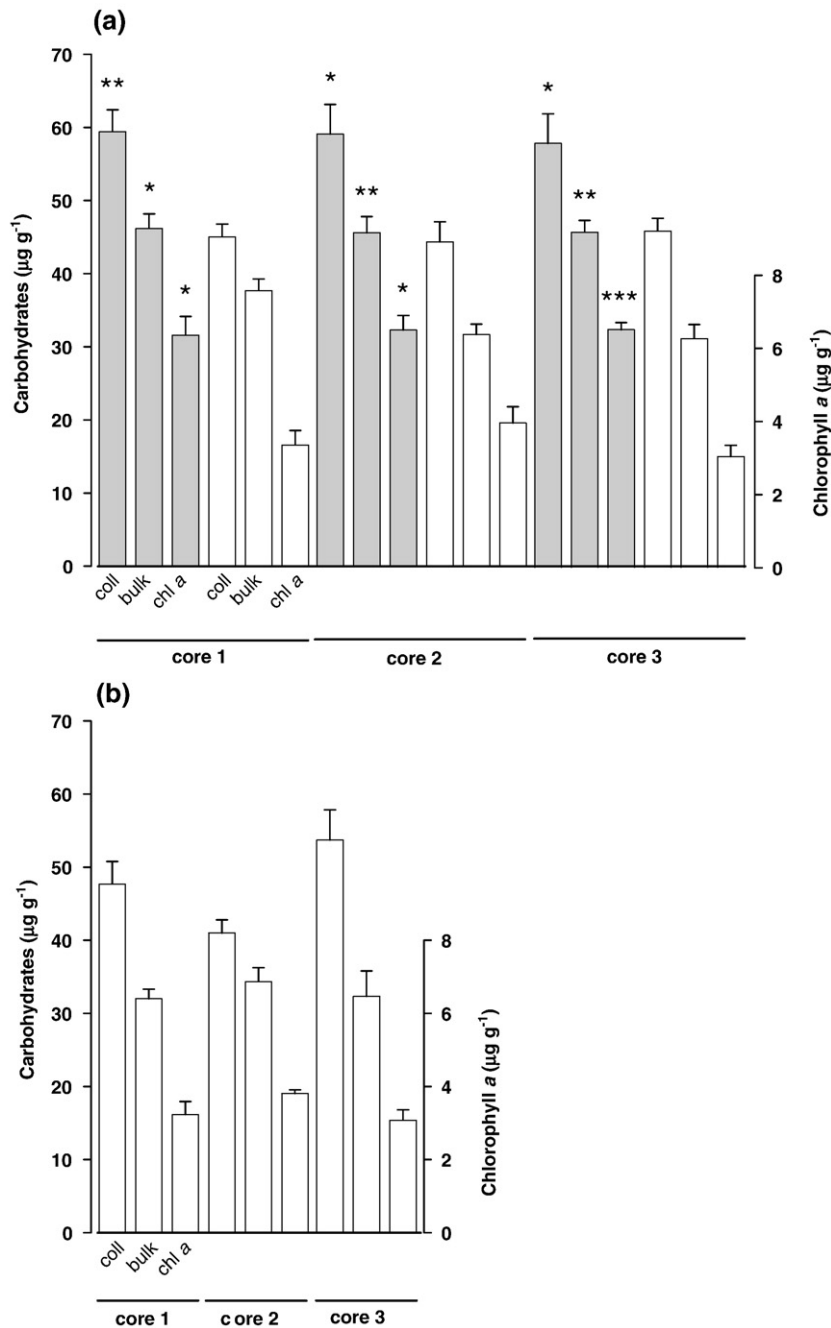


Fig. 2. The concentration of colloidal and bulk carbohydrates, and chlorophyll *a* in surface sediments (0–1 cm) from mini-cores sampled from Plexiglas™ cores at sites 1, (a) and 2, (b). Grey bars indicate sediments collected beneath microbial mats and open bars indicate no mat cover. Plotted values are means \pm S.E. ($n=3$). Comparison tests of surface sediments at site 1 (a), using paired *t*-test analysis within cores containing microbial mats and bare sediment show significant differences indicated as * <0.05 , ** <0.01 , *** <0.001 .

intervals at incremental speeds from 14–40 rpm (representing u^* of 0.9 to 2.0 cm s^{-1}). The onset of sediment erosion was detected via turbidity and videography.

Turbidity was monitored to quantify erosion rate via % transmission with a fiber-optic spectrophotometer (Brinkmann PC 800 colorimeter, 670 nm) mounted in the Plexiglas™ core above the perforated grid. To determine the SPM concentrations the probe was zeroed with filtered seawater and calibrated with a series of increasing concentration using sediment from the site. The exact concentrations of the calibration samples were determined using GF/F filters, drying and weighing. The filtrate of suspended particulate matter (SPM) was retained for analysis of organic content.

Calibration of the turbidity probe using sediment from both sites produced strong linear relationships between SPM and % transmission ($r^2=0.83$ site 1; $r^2=0.82$ site 2). However there may be potential errors in calibrating the probe post-erosion sequence, as optical turbidity sensors are sensitive to such factors as particle size spectrum, colour of the particles and photosynthetic pigment contents, all of which may have altered during erosion. Erosion rates (quantity of material eroded), expressed as $\text{g sediment m}^{-2} \text{ s}^{-1}$ were calculated for each motor interval based on regression analysis of the sediment turbidity and SPM calibration curves from each site.

Sediment erosion experiments were standardized by selecting an initial oscillating speed of 14 rpm. The oscillating

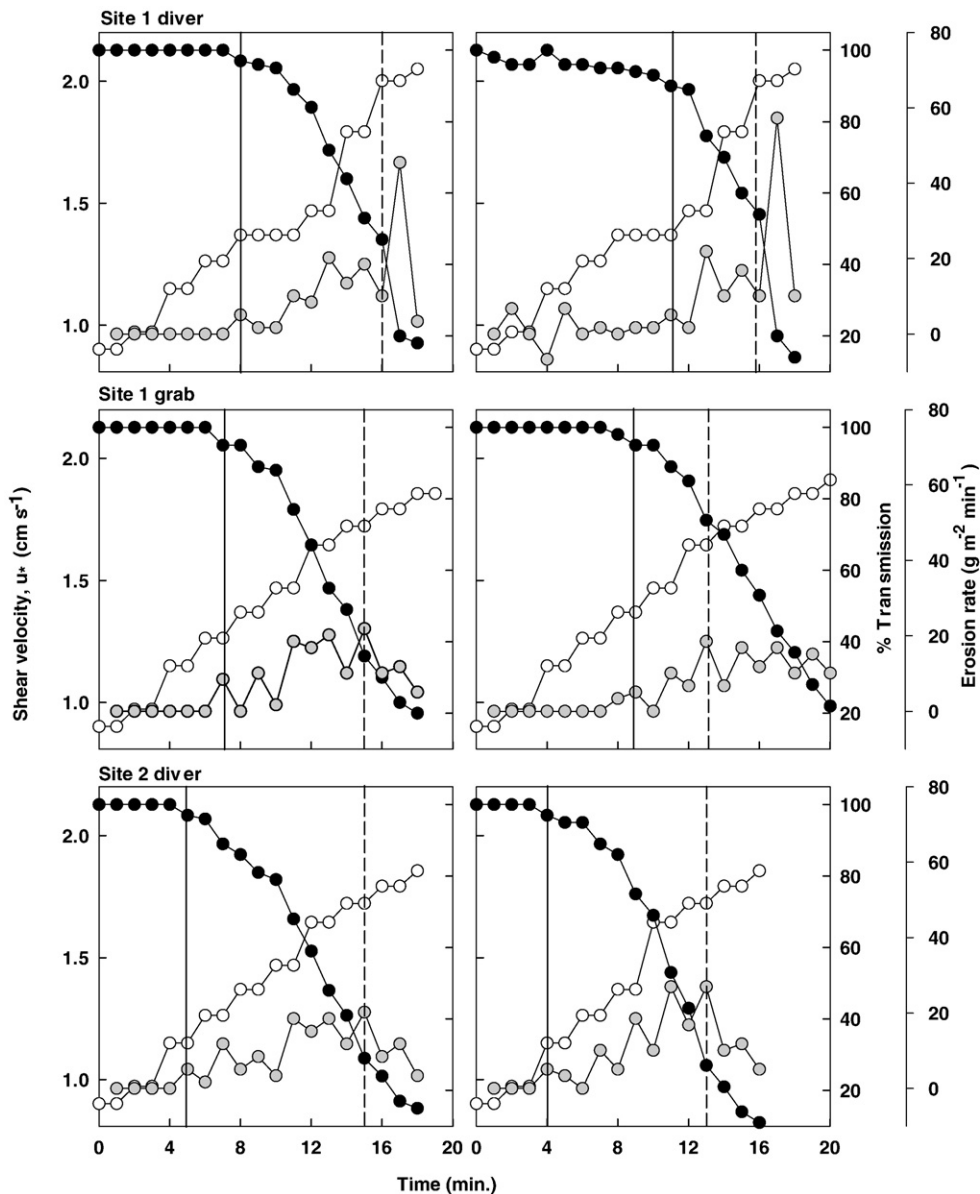


Fig. 3. Representative duplicate examples of time series of erosion sequences generated by the PES showing shear velocity (○), % transmission (●) and erosion rate expressed as mass of material eroded (●) against experiment duration for site 1 using diver cores (top); site 1 using grab cores (middle); site 2 using diver cores (bottom). The onset of erosion is indicated by the vertical solid line (the point at which turbidity begins to increase), whereas the onset of significant erosion (critical shear velocity) is indicated by the vertical dashed line.

grid frequency was then increased by 1–2 rpm at 2 min intervals. Visual observations of erosion events within the core were noted at 1 min intervals and the sequence of sediment erosion was also recorded using a mini-digital camcorder (model Canon ZR45 MC) with still images captured using digital capture software (Pinnacle Studio) (Walker et al., in press). Particle size distributions were also determined from these images using SigmaScan Pro version 5 (SPSS Inc.). A scale bar on the outside of the core was used to calibrate images and the minimum particle size expressed as Estimated Spherical Diameter (ESD) measured using this technique was 100 μm . Parallax and depth of field distortions were corrected for by using beads of known size (500 μm). The core water column became too turbid for particle discrimination at greater than 30 rpm ($u^* = 1.79 \text{ cm s}^{-1}$). A digital still camera held above cores followed by image analysis was used to record microbial mat surface area.

3. Results

3.1. Sediment properties

At site 1 the sieve contents $>250 \mu\text{m}$ consisted of *Z. marina* (Eelgrass) detritus and mussel shell fragments. Sediments were described as muddy sand, comprising of 81% sand and 19% mud ($D_{50} = 120 \mu\text{m}$) with porosities of 70%. Sediments were high in organic content and TOC with a mean C/N ratio of 7.8 (Table 1). The sediment surface area comprised substantial microbial mats ($48\% \pm 4.4 \text{ SE } n = 12$) consisting of white sulfur bacteria and cyanobacteria but few obvious macro-fauna. There is a tendency toward sub-oxic conditions in these sediments with pore water sulfides $\sim 2500 \mu\text{mol}$. Site 2 was more oxygenated as indicated by pore water sediment sulfides $<1000 \mu\text{mol}$ (B. Hargrave, Bedford Institute of Oceanography, Department of Fisheries and Oceans, personal communication). Site 2 was sandier with 87% of the bulk composition in the 250 μm class accounting for the coarser texture at this site ($D_{50} = 316 \mu\text{m}$). Sediment organic content and TOC were about 30% less than site 1, although C/N ratios were similar (Table 1). No microbial mats were observed but macro-fauna were present.

3.2. Sedimentary carbohydrates and chlorophyll *a*

Concentrations of colloidal and bulk carbohydrates, and chlorophyll *a* at site 1 below microbial mats were: 60, 47 and $5.5 \mu\text{g g}^{-1}$ respectively. These values were significantly greater than for exposed sediment at the same site (no mat cover; 46, 37 and $4.0 \mu\text{g g}^{-1}$ respectively; Fig. 2a) (paired *t*-test, $P < 0.05$ in all cases). In the absence of any microbial mats at site 2, concentrations of colloidal and bulk carbohydrates, and chlorophyll *a* were: 48, 30 and $3.2 \mu\text{g g}^{-1}$ respectively. These were no different from the concentrations found in exposed sediment at site 1 (*t*-test, $P > 0.05$ in all cases) (Fig. 2b).

3.3. Critical shear velocity and erosion rates

Critical shear velocities for the purposes of this study were defined as the point at which the onset of significant erosion was observed in the cores (L. Sandford, Horn Point Environmental Laboratory, University of Maryland, personal communication),

whereas the onset of erosion was defined as the point at which turbidity began to increase. This was confirmed by a combination of our largely subjective real time observations, turbidity measurements, videography and erosion sequences (see Fig. 3). Quantitative analysis of cores from site 1 indicates that mean critical shear velocities for cores collected by divers and grabs was 1.77 cm s^{-1} ($\pm 0.08 \text{ SE}$, $n = 6$) and 1.70 cm s^{-1} ($\pm 0.06 \text{ SE}$, $n = 6$) respectively (Fig. 3). No significant differences were observed between mean critical shear velocities for either method of core collection (*t*-test, $P > 0.05$). At site 2 the mean critical shear velocity (diver collection only) was not significantly different from site 1 ($1.75 \text{ cm s}^{-1} \pm 0.07 \text{ SE}$, $P > 0.1$, $n = 3$; Fig. 3), but the sequence of erosion was distinctly different at the two sites owing to the presence of microbial mats at site 1. The record of turbidity within cores at site 1 displayed consistently lower values but at about the fifth motor speed increment, there is a slight rise in turbidity as erosion began (Fig. 3). Visual field observations indicate that this corresponds to the point when the mat began to fail and underlying unconsolidated sediments are resuspended which were observed as small particles ($<1 \text{ mm}$) lifting from the bed (Fig. 4). When further stress was applied we observed complete failure of the bed and critical erosion was achieved when the suspension became fully turbid. The shear stress applied to the sediment was sufficient to lift larger particles and maintain them in suspension with several particle size classes represented between 0.3 and $>3 \text{ mm}$ (Fig. 5). The lowest % transmission in cores collected from site 1 corresponded to a range of SPM concentration from 2700 to 5312 mg L^{-1} .

These erosion sequences were quite different from cores at site 2 where erosion began at speed step 3 or 4 (Fig. 3). The gradual erosion sequences at site 2 made the determination of critical erosion threshold more subjective. In cores from site 2, small particles ($<1 \text{ mm}$) began to lift from the bed at the fourth motor speed increment. For cores collected from site 2 the range of SPM observed in the cores was from 3520 to 5376 mg L^{-1} . The greatest material eroded from each run was recorded up to $71 \text{ g m}^{-2} \text{ min}^{-1}$ for site 1 (mean $= 47 \pm 5.9$), which was significantly different from the values observed at site 2 (maximum $= 26 \text{ g m}^{-2} \text{ min}^{-1}$; mean $= 23 \pm 3.6$; *t*-test, $P < 0.001$).

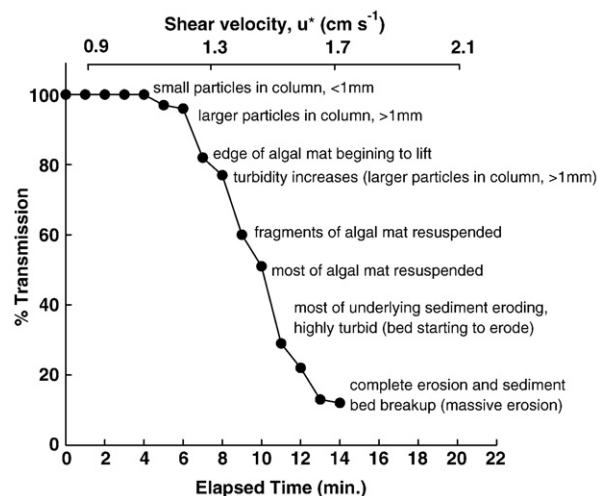


Fig. 4. Typical field observations on sediment bed erosion with increasing shear velocity from site 1 and 2 (with observations for site 2 in parenthesis).

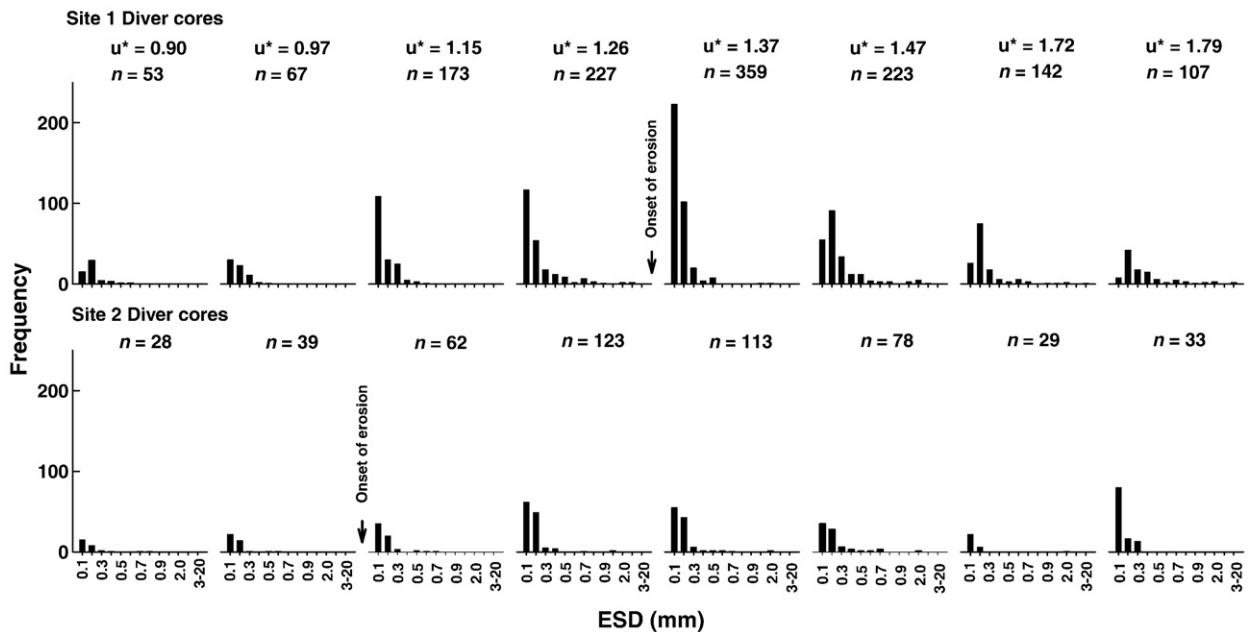


Fig. 5. Mean particle size frequency, using ESD (mm) measured at different bed shear velocities on bottom sediments at sites 1 and 2 using diver cores ($n=3-6$).

The frequency distribution of resuspended particle sizes for the various cores ranged from the lower limit of detection, 100 μm to 1700 μm for both sites and methods of coring (mean = 180 $\mu\text{m} \pm 8$ SE, $n=3,512$) at different erosion thresholds (Fig. 5). There appeared to be no difference in particle frequency and size distribution between both methods of collection at site 1 and so ESD frequency distributions are shown for diver cores at site 1 only. However, at site 2 there appeared to be fewer particles in suspension at each erosion sequence (as evidenced by the ESD frequency distributions in Fig. 5) probably reflecting that site's coarser grain size. The pattern of particle size frequencies at site 1 initially showed fewer particles eroding at lower shear velocities all within the smallest size classes. However, as shear velocity increased, there was a dramatic increase in number and size of particles as microbial mats began to erode. This confirmed observations made during erosion experiments where particles did not resuspend until microbial mats began to lift at the edges. With increased shear velocities the mats began to break off at the edges causing large fragments of microbial material to be resuspended. Once microbial mats were lifted or began breaking up fine sediment particles were easily resuspended by the oscillating grid and bed erosion occurred at the exposed sediment surface. At site 2 in the absence of microbial mats particle sizes remained more consistent throughout the erosion sequences but absolute numbers of particles increased with increasing shear velocity until turbidity became a limiting factor for counting.

Image analysis of captured stills shows a strong positive relationship between mean ESD and sediment surface shear velocity from cores collected at site 1 by divers and grabs ($r^2=0.63$) and there was no significant difference between the slopes of these curves (ANCOVA: $F=0.67$, $P=0.429$, $n=12$; Fig. 6a). There was no corresponding relationship observed between ESD and shear velocity at site 2 ($r^2=0.08$) (Fig. 6b). Visual observations of erosion sequences confirmed variance in floc size increased with the presence of larger aggregates

likely because they have a shorter residence time in the field of view, as a result of their subsequent break down into smaller flocs with increasing turbulence.

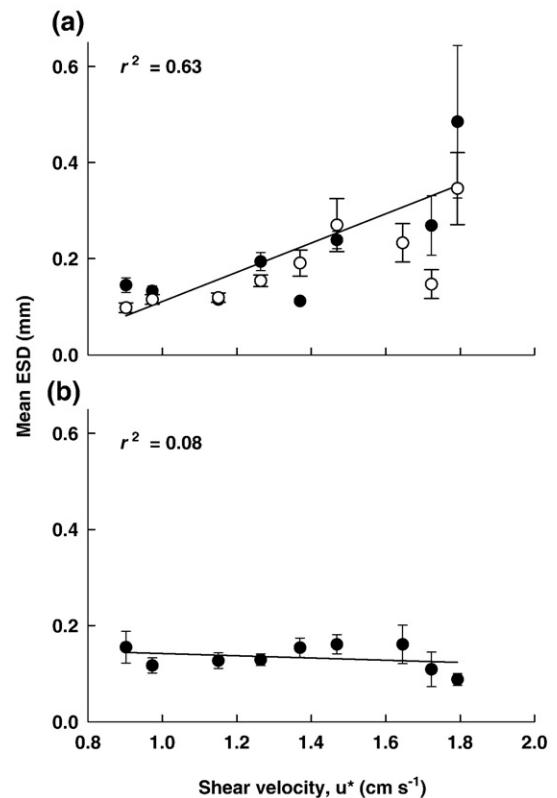


Fig. 6. Relationship between mean ESD (mm) and sediment surface shear velocity (cm s^{-1}) from site 1 (a) and site 2 (b) collected by divers (●) and grab cores (○). Plotted values are means \pm S.E. ($n=42-428$).

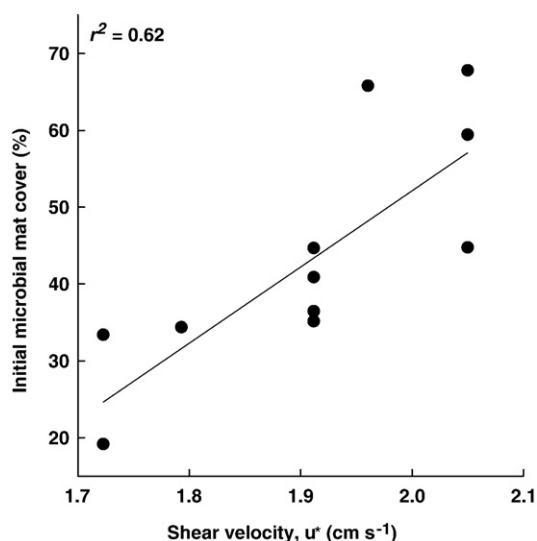


Fig. 7. Relationship between initial microbial mat surface area and shear velocity for cores at site 1 ($n=11$).

Mats never reached full coverage at site 1 (48 ± 4.4) and cores with less armoring by mats had lower critical shear velocities. Although the range of critical shear velocities was small there was a strong positive relationship between microbial mat surface area and shear velocity for cores at site 1 ($r^2=0.62$; $n=12$; Fig. 7).

4. Discussion

There are a number of difficulties associated with quantitative prediction of the erodibility of sediments. These include the variety of erosion devices available and the different protocols used to calculate the derived erosion parameters (Sanford and Maa, 2001; Sanford, 2006). Our results demonstrate that the re-designed PES serves as useful proxy for sediment erosion by quantifying multiple variables such as, erosion rate and particle size analysis (Walker et al., submitted for publication). The clear Plexiglas™ cores allowed for detailed observations of sediment erosion, along with simultaneous measurements of turbidity and particle size analysis.

Analysis of cores from site 1 indicated that the critical shear velocities for both methods of core collection (diving and grabs) were not significantly different and demonstrated that intact sediment cores can be assessed for sediment erosion using either method of collection in the field. This finding is important for applications of this methodology to greater depths or ice-choked waters where diving is not feasible such as the Beaufort Sea (e.g. Walker et al., in press).

Surprisingly there were also no significant differences in critical shear velocities between sites despite the contrasting nature of these two locations. For example, the coarser sediment texture at site 2 may have been important in defining erosion parameters for this location compared to the initial biostabilization by microbial mats at site 1. Despite the similarities, the observed sequence of erosion was distinctly different at the two sites owing to the presence of microbial mats at site 1. This observation was expressed as a significant difference in the mass of eroded material between sites. The

lower suspended sediment mass in site 2 experiments may have been because there was less fine sediment available there. The material suspended at site 2 was considerably finer than the material in the bed. The larger sand grains in the bed that was not suspended probably armored the bed, limiting continued erosion of the finer material. This also explains the decreasing erosion rates toward the end of all site 2 erosion sequences. Therefore, deriving the critical shear velocity from the mass of sediment eroded may also detect differences between sites not detectable using the transmission probe alone.

Erosion was observed at both sites; however, the transition between them was more dramatic at site 1 where microbial mats mediated resuspension processes. At site 1 sediment beds were armored by microbial mats until a point at which they failed, causing subsequent resuspension of the underlying sediment. Erosion rate calculations respond to small changes in turbidity at each time interval and were a sensitive indicator of instantaneous resuspension. As erosion began, there was a steep rise in erosion rate with increasing stress scouring more of the unconsolidated layer. As erosion continued the greatest amount of material was resuspended as the bed eroded cohesive sediments which yielded fewer and larger particles, probably explaining the jagged shape of the erosion rate curves. For example, the turbidity when the shear stress had just been increased was usually not much higher because the increased shear stress had not yet had time to respond, so the derived erosion rate at that time interval was relatively low. By the next time interval, the higher stress had eroded more material and the derived erosion rate was therefore higher. These observations reiterate previous studies which demonstrated multiple erosion rates were dependent on sediment texture and the vertical distribution of shear strength (Amos et al., 1992; Tolhurst et al., 2000).

One of the primary impacts of mussel culture is enhanced sedimentation or biodeposition of fecal and pseudofecal material (Chamberlain et al., 2001). The ecological impacts of this increased sedimentation are organic loading, sediment hypoxia, eutrophication and altered macro-faunal communities (Hatcher et al., 1994; Callier et al., 2006). Among the many environmental responses to intensive mussel culture are the development of microbial mats, increased levels of particulate organic matter (POM), and the decline in benthic invertebrate biodiversity (Stenton-Dozey et al., 1999; Newell, 2004). Grant et al. (2005) demonstrated that sedimentation rates were double at mussel sites compared to sites less affected by longline culture in Tracadie Bay. Despite the increased biodeposition sediments at site 1 did not have a flocculent layer as expected from this deposition. Due to the care of diver collection we knew that there were no disturbance artifacts associated with this observation. In contrast, Giles and Pilditch (2004) found that organic-rich biodeposits from mussels forming a flocculent layer were easily eroded at shear velocities below 1 cm s^{-1} . Another study by Lelieveld et al. (2004) found mean critical shear velocity values of 1.5 cm s^{-1} in sediments with high densities of the deposit feeding bivalve, *Macomona liliana* which were in the same range as those reported here.

In our study biodeposits at site 1 were either dispersed (rather than sedimented) or incorporated into the microbial mat structure itself. Cores containing large areas of mat were

effectively biostabilized, producing an armoring effect of the underlying sediment, which was evident from the relationship between mat coverage and shear velocity. Microbial mats were typically patchy and our study was one of a few to demonstrate that the spatial coverage is directly related to resuspendability. The implication of a single value of critical shear velocity is difficult to apply to large areas without some weighting for the extent of mat coverage which was beyond the scope of this study. Similarly, Grant and Gust (1987) were able to show that the 'carpet' erosion of cyanobacterial mats in a laboratory flume had a strong relationship with sediment chlorophyll *a* content in the upper 2 mm of exposed sediment. Their study found that cyanobacterial stabilization achieved critical shear velocities of 4 cm s^{-1} , which were far in excess of those found in this study, but cores with a 'clear' surface in their study were eroded at critical shear velocities below 1.3 cm s^{-1} comparable to shear velocities found with bare sediments at site 2. Studies by Paterson (1989) and Lintern et al. (2002) also found that sediments underlying biofilms (once exposed), were more easily eroded than the biostabilized layers. Mehta and Christensen (1983) and Nizzoli et al. (2005) found that additional stabilization could also be brought about in sediments by a matrix of shells and shell fragments which were abundant in Tracadie Bay as a result of the extensive mussel culture.

Using an *in situ* benthic annular flume Thompson et al. (2004) found that sediments were effectively biostabilized by *Z. marina* (Eelgrass) beds in Rustico Bay, an adjacent embayment in PEI. Although *Z. marina* was common in Tracadie Bay none were found in cores used for our erosion experiments. Quantification using a Biostabilization Index (BI) on sediments in Venice Lagoon, Amos et al. (2004) found that sediment beds covered by filamentous cyanobacteria had a BI of 244% compared to sediments covered by the local *Z. noltii* (Seagrass) which had a slightly lower BI of 206%. They also found that bare sublittoral sediment beds were the least resistant with a BI of 58%, which was apparent in our cores from site 2 with bare sediment during the initial stages of erosion.

Sutherland et al. (1998a) and Lelieveld et al. (2004) were also able to show how sediment erosion rates increased with higher concentrations of sediment chlorophyll *a* and carbohydrates using flume experiments. Chlorophyll *a* and carbohydrate content of organic-rich sediments in Tracadie Bay was relatively low despite the presence of benthic microbial mats although differences were observed in chlorophyll *a* and carbohydrate concentrations between sediments underlying microbial mats at site 1 and exposed sediments at site 2. Paterson (1989) noted that diatom biofilms were limited to the topmost 2 mm of sediments, and it was therefore possible that the chlorophyll *a* and carbohydrate content may have been underestimated in this study by the dilution effect of sampling down to 1 cm, which included the microbial mat-free underlying sediment. Chlorophyll *a* and colloidal and bulk carbohydrate concentrations in these subtidal sediments were comparable to those in intertidal sandflats and subtidal sediments in Nova Scotia observed by Grant et al. (1986) and Sutherland et al. (1998b). The subtidal sediments in our study showed no obvious relationship between sediment chlorophyll *a* and colloidal carbohydrate concentrations for both sites which could be due to a decrease in algal pigments as the mats were predominantly bacterial or because of the small range of sites sampled.

The strong relationship between microbial mat surface area and shear velocity at site 1 further demonstrated the cohesive properties of biofilms in stabilizing sediments but it is interesting to note that once exposed these sediments were eroded by identical shear velocities as site 2. Particle size distribution of resuspended sediments was dependent on the stage of erosion and failure of microbial mats. Sutherland et al. (1998a) observed similar erosion of large aggregates (10–15 mm diameter) when erosion experiments were performed on diatom mats, which were in the same size class of the largest aggregates observed in this study. Other studies have shown that the effect of SPM concentration on particle size remains unclear, especially when biological aggregates are resuspended (e.g. Dyer et al., 2004). The influence of turbulent shear on aggregates in the water column is particularly important since it affects their residence time in the water column and ability to interact in benthic–pelagic coupling. It is apparent that mussel aquaculture impacts the erodibility of sediments in Tracadie Bay although we did not observe a fluff layer that might have been expected under these conditions. However, other impacts such as nutrients excreted by mussels may be important in the development of microbial mats and their effects on sediment texture (Newell, 2004). Using these critical shear stress and erosion rate values it may be possible to predict periods of erosion due to tidal or wind generated bottom flow. This information coupled with patchiness in sediment erodibility and particle size distribution could be collated to model resuspension in systems like Tracadie Bay, where mussel culture has a large influence on particle dynamics (Grant et al., 2005).

The re-designed and calibrated PES has shown that it can be used for quantifying sediment erosion offshore in the Arctic and in shallow subtidal sediments subject to benthic impacts from mussel culture (Walker et al., *in press*). It has also been further validated by comparing two methods of sediment sample collection in this study. Sediment integrity was maintained when using push cores from SCUBA divers or grabs and both methods can be used to obtain intact sediment cores for future assessments. The diversity of information obtained using the PES (critical threshold, erosion rate, particle size distribution) provides much of the required information for assessing the role of resuspension in particle cycling in coastal and shelf environments.

5. Conclusions

The portable PES device has been shown to be a useful proxy of sediment erosion for field deployments in coastal ecosystems. Two contrasting sites had similar critical shear velocities despite differences in sediment properties. Microbial mats resulting from mussel culture impacts effectively 'armored' soft sediments and biostabilized sediments.

Acknowledgements

This work formed part of the CASES project (Canadian Arctic Shelves Exchange Study), a Research Network funded by the Natural Sciences and Engineering Research Council of Canada (NSERC). We wish to thank Peter Cranford for his skillful boat maneuvering and Shelley Armsworthy and Janie Jones for collecting sediment cores using SCUBA. We would also like to thank Paul MacPherson for CHN analysis and

Marie-Claude Archambault for help in the field lab. We also greatly appreciate insightful comments from L. Sanford, D.G. Lintern and an anonymous reviewer whose comments helped improve this paper.

References

- Amos, C.L., Grant, J., Daborn, G.R., Black, K., 1992. Sea Carousel—a benthic, annular flume. *Estuar. Coast. Shelf Sci.* 34, 557–577.
- Amos, C.L., Bergamasco, A., Umgiesser, G., Cappucci, S., Cloutier, D., DeNat, L., Flindt, M., Bonardi, M., Cristante, S., 2004. The stability of tidal flats in Venice Lagoon — the results of in-situ measurements using two benthic, annular flumes. *J. Mar. Syst.* 51 (1–4), 211–241.
- Callier, M.D., Weise, A.M., McKindsey, C.W., Desrosiers, G., 2006. Sedimentation rates in a suspended mussel farm (Great-Entry Lagoon, Canada): biodeposit production and dispersion. *Mar. Ecol. Prog. Ser.* 322, 129–141.
- Chamberlain, J., Fernandes, T.F., Read, P., Nickell, T.D., Davies, I.M., 2001. Impacts of deposits from suspended mussel (*Mytilus edulis* L.) culture on the surrounding surficial sediments. *ICES J. Mar. Sci.* 58, 411–416.
- Dade, B.W., Davis, J.D., Nichols, P.D., Nowell, A.R.M., Thistle, D., Trexler, M.B., White, D.C., 1990. Effects of bacterial exopolymer adhesion on the entrainment of sand. *Geomicrobiol. J.* 8, 1–16.
- Dowd, M., 2005. A bio-physical coastal ecosystem model for assessing environmental effects of marine bivalve aquaculture. *Ecol. Model.* 183, 323–346.
- Dyer, K.R., Christie, M.C., Manning, A.J., 2004. The effects of suspended sediment on turbulence within an estuarine turbidity maximum. *Estuar. Coast. Shelf Sci.* 59, 237–248.
- Giles, H., Pilditch, C.A., 2004. Effects of diet on sinking rates and erosion thresholds of mussel *Perna canaliculus* biodeposits. *Mar. Ecol. Prog. Ser.* 282, 205–219.
- Grant, J., Emerson, C.W., 1995. Resuspension and stabilization of sediments with microbial biofilms, implications for benthic–pelagic coupling. In: Krumbein, W.E., Paterson, D.M., Stal, L.J. (Eds.), *Biostabilization of Sediments*. Verlag Rosemeier, Bad Zwischenahn, pp. 121–134.
- Grant, J., Gust, G., 1987. Prediction of coastal sediment stability from photopigment content of mats of purple sulphur bacteria. *Nature* 330, 244–246.
- Grant, J., Mills, E.L., Hopper, C.M., 1986. A chlorophyll budget of the sediment–water interface and the effect on stabilizing biofilms on particle fluxes. *Ophelia* 26, 207–219.
- Grant, J., Hargrave, B.T., MacPherson, P., 2002. Sediment properties and benthic–pelagic coupling in the North Water. *Deep-Sea Res.* II 49, 5259–5275.
- Grant, J., Cranford, P., Carreau, M., Schofield, B., Armsworthy, S., Burdett-Coutts, V., Ibarra, D., 2005. A model of aquaculture impacts for multiple estuaries and its field verification at mussel culture sites in Eastern Canada. *Can. J. Fish. Aquat. Sci.* 62, 1271–1285.
- Hatcher, A., Grant, J., Schofield, B., 1994. Effects of suspended mussel culture (*Mytilus* spp.) on sedimentation, benthic respiration and sediment nutrient dynamics in a coastal bay. *Mar. Ecol. Prog. Ser.* 115, 219–235.
- Lelieveld, S.D., Pilditch, C.A., Green, M.O., 2003. Variation in sediment stability and relation to indicators of microbial abundance in the Okura Estuary, New Zealand. *Estuar. Coast. Shelf Sci.* 57, 123–136.
- Lelieveld, S.D., Pilditch, C.A., Green, M.O., 2004. Effects of deposit-feeding bivalve (*Macomona liliana*) density on intertidal sediment stability. *N.Z. J. Mar. Freshw. Res.* 38, 115–128.
- Lintern, D.G., Sills, G.C., Feates, N., Roberts, W., 2002. Erosion properties of mud beds deposited in laboratory settling columns. In: Winterwerp, J.C., Kranenburg, C. (Eds.), *Fine Sediment Dynamics in the Marine Environment*. Proceedings in Marine Sciences. Elsevier, pp. 343–357.
- Lorenzen, C.J., 1967. Determination of chlorophyll and pheopigments: spectrophotometric equations. *Limnol. Oceanogr.* 12, 343–346.
- Lucas, M.I., Newell, R.C., Velimirov, B., 1981. Heterotrophic utilization of mucilage released during fragmentation of kelp (*Ecklonia maxima* and *Laminaria pallida*). II. Differential utilization of dissolved organic components from kelp mucilage. *Mar. Ecol. Prog. Ser.* 4, 43–55.
- Lucas, C.H., Widdows, J., Wall, L., 2003. Relating spatial and temporal variability in sediment chlorophyll *a* and carbohydrate distribution with erodibility of a tidal flat. *Estuaries* 26, 885–893.
- Madsen, K.N., Nilsson, P., Sundbäck, K., 1993. The influence of benthic microalgae on the stability of a subtidal sediment. *J. Exp. Mar. Biol. Ecol.* 170, 159–177.
- Meeuwig, J.J., Rasmussen, J.B., Peters, R.H., 1998. Turbid waters and clarifying mussels: their moderation of empirical chl:nutrient relations in estuaries in Prince Edward Island, Canada. *Mar. Ecol. Prog. Ser.* 171, 139–150.
- Mehta, A.J., Christensen, B.A., 1983. Initiation of sand transport over coarse beds in tidal entrances. *Coast. Eng.* 7, 61–75.
- Newell, R.I.E., 2004. Ecosystem influences of natural and cultivated populations of suspension-feeding bivalve molluscs: a review. *J. Shellfish Res.* 23, 51–61.
- Nizzoli, D., Welsh, D.T., Bartoli, M., Viaroli, P., 2005. Impact of mussel (*Mytilus galloprovincialis*) farming on oxygen consumption and nutrient recycling in an eutrophic coastal lagoon. *Hydrobiologia* 550, 183–198.
- Parsons, T.R., Maita, Y.I., Lalli, C.M., 1984. *A Manual of Chemical and Biological Methods for Seawater Analysis*. Pergamon.
- Paterson, D.M., 1989. Short-term changes in the erodibility of intertidal cohesive sediments related to the migratory behavior of epipellic diatoms. *Limnol. Oceanogr.* 34, 223–234.
- Paterson, D.M., Crawford, R.M., Little, C., 1990. Subaerial exposure and changes in the stability of intertidal estuarine sediments. *Estuar. Coast. Shelf Sci.* 30, 541–556.
- Sanford, L.P., 2006. Uncertainties in sediment erodibility estimates due to a lack of standards for experimental protocols and data interpretation. *Integr. Environ. Assess. Manag.* 2 (1), 29–34.
- Sanford, L.P., Maa, J.P.-Y., 2001. A unified erosion formulation for fine sediments. *Mar. Geol.* 179 (1–2), 9–23.
- Shaw, K.R., 1998. PEI benthic survey. Technical Report of Environmental Sciences, No. 4, Department of Environment and Department of Fisheries and Environment, 75 pp.
- Stenton-Dozey, J.M.E., Jackson, L.F., Busby, A.J., 1999. Impact of mussel culture on macrobenthic community structure in Saldahana Bay, South Africa. *Mar. Pollut. Bull.* 39, 357–366.
- Sutherland, T.F., Grant, J., Amos, C.L., 1998a. The effect of carbohydrate production by the diatom *Nitzschia curvilineata* on the erodibility of sediment. *Limnol. Oceanogr.* 43, 65–72.
- Sutherland, T.F., Amos, C.L., Grant, J., 1998b. The effect of buoyant biofilms on the erodibility of sublittoral sediments of a temperate microtidal estuary. *Limnol. Oceanogr.* 43, 225–235.
- Thompson, C.E.L., Amos, C.L., Umgiesser, G., 2004. A comparison between fluid shear stress reduction by halophytic plants in Venice Lagoon, Italy and Rustico Bay, Canada — analyses of *in situ* measurements. *J. Mar. Syst.* 51 (1–4), 293–308.
- Tolhurst, T.J., Black, K.S., Paterson, D.M., Mitchener, H.J., Termaat, G.R., Shayler, S.A., 2000. A comparison and measurement standardization of four *in situ* devices for determining the erosion shear stress of intertidal sediments. *Cont. Shelf Res.* 20, 1397–1418.
- Tsai, C.-H., Lick, W., 1986. A portable device for measuring sediment resuspension. *J. Great Lakes Res.* 12, 314–321.
- Walker, T.R., 2005. Vertical organic inputs and bio-availability of carbon in an Antarctic coastal sediment. *Pol. Polar Res.* 26 (2), 91–106.
- Walker, T.R., Grant, J., Hill, P.S., Lintern, D.G., submitted for publication. BEAST—a portable device for quantification of erosion in intact sediment cores. *Limnol. Oceanogr. Meth.*
- Walker, T.R., Grant, J., Cranford, P., Lintern, D.G., Hill, P.S., Jarvis, P., Barrel, J., Nozais, C., in press. Suspended sediment and erosion dynamics in Kugmallit Bay and Beaufort Sea during ice-free conditions. *J. Mar. Syst.* doi:10.1016/j.marsys.2008.01.006.
- Watts, C.W., Tolhurst, T.J., Black, K.S., Whitmore, A.P., 2003. *In situ* measurements of erosion shear stress and geotechnical shear strength of the intertidal sediments of the experimental managed realignment scheme at Tollesbury, Essex, UK. *Estuar. Coast. Shelf Sci.* 58, 611–620.
- Widdows, J., Brinsley, M.D., Bowley, N., Barrett, C., 1998. A benthic annular flume for *in situ* measurement of suspension feeding/biodeposition rates and erosion potential of intertidal cohesive sediments. *Estuar. Coast. Shelf Sci.* 46, 27–38.